NEP1-40 promotes myelin regeneration via upregulation of GAP-43 and MAP-2 expression after focal cerebral ischemia in rats

HONG ZHAO[1], ZHEN-DONG LIU[2], YONG-BO ZHANG[3], XIAO-YU GAO[4], CUI WANG[1], YI LIU[1] and XUN-FEN WANG[5]

[1]Department of Neurology, Dalian Municipal Central Hospital Affiliated to Dalian Medical University, Dalian, Liaoning 116033; [2]Department of General Medicine, Central Hospital Affiliated to Shaoxing University, Shaoxing, Zhejiang 312000; [3]Department of Neurology, Beijing Friendship Hospital, Capital Medical University, Beijing 100050; [4]Department of Neurology, The Affiliated Yantai Yuhuangding Hospital of Qingdao University, Yantai, Shandong 264000; [5]Department of Neurology, Dalian Medical University, Dalian, Liaoning 116033, P.R. China

Received June 10, 2021; Accepted September 8, 2021

DOI: 10.3892/mmr.2021.12484

Abstract. Axon regeneration after lesions to the central nervous system (CNS) is largely limited by the presence of growth inhibitory molecules expressed in myelin. Nogo-A is a principal inhibitor of neurite outgrowth, and blocking the activity of Nogo-A can induce axonal sprouting and functional recovery. However, there are limited data on the expression of Nogo-A after CNS lesions, and the mechanism underlying its influences on myelin growth remains unknown. The aim of the present study was to observe the time course of Nogo-A after cerebral ischemia/reperfusion in rats using immunohistochemistry and western blot techniques, and to test the effect of its inhibitor Nogo extracellular peptide 1-40 (NEP1-40) on neural plasticity proteins, growth-associated binding protein 43 (GAP-43) and microtubule associated protein 2 (MAP-2), as a possible mechanism underlying myelin suppression. A classic model of middle cerebral artery occlusion (MCAO) was established in Sprague-Dawley rats, which were divided into three groups: i) MCAO model group; ii) MCAO + saline group; and iii) MCAO + NEP1-40 group. Rats of each group were divided into five subgroups by time points as follows: days 1, 3, 7, 14 and 28. Animals that only received sham operation were used as controls. The Nogo-A immunoreactivity was located primarily in the cytoplasm of oligodendrocytes. The number of Nogo-A immunoreactive cells significantly increased from day 1 to day 3 after MCAO, nearly returning to the control level at day 7, increased again at day 14 and decreased at day 28. Myelin basic protein (MBP) immunoreactivity in the ipsilateral striatum gradually decreased from day 1 to day 28 after ischemia, indicating myelin loss appeared at early time points and continuously advanced during ischemia. Then, intracerebroventricular infusion of NEP1-40, which is a Nogo-66 receptor antagonist peptide, was administered at days 1, 3 and 14 after MCAO. It was observed that GAP-43 considerably increased from day 1 to day 7 and then decreased to a baseline level at day 28 compared with the control. MAP-2 expression across days 1-28 significantly decreased after MCAO. Administration of NEP1-40 attenuated the reduction of MBP, and upregulated GAP-43 and MAP-2 expression at the corresponding time points after MCAO compared with the MCAO + saline group. The present results indicated that NEP1-40 ameliorated myelin damage and promoted regeneration by upregulating the expression of GAP-43 and MAP-2 related to neuronal and axonal plasticity, which may aid with the identification of a novel molecular mechanism of restriction in CNS regeneration mediated by Nogo-A after ischemia in rats.

Introduction

The capacity for the adult brain to repair itself by axonal regeneration or compensatory fiber growth following hypoxia/ischemia is extremely limited and incomplete, partly due to several factors, including glial scars, lack of neurotrophins and inhibitory proteins that create a non-permissive environment and limit the structural plasticity of injured neurons (1). It has been reported that three myelin-associated proteins, Nogo-A, myelin-associated glycoprotein and oligodendrocyte myelin glycoprotein, are implicated as inhibitors of axonal growth (2). Among them, Nogo-A cloned in 2000 has received much attention as a major obstacle to successful axon regeneration (3). Nogo-A, a reticulon protein family member, is widely localized in the cell bodies of oligodendrocytes and in

Correspondence to: Professor Hong Zhao, Department of Neurology, Dalian Municipal Central Hospital Affiliated to Dalian Medical University, 826 Xi Nan Road, Dalian, Liaoning 116033, P.R. China
E-mail: zhaohong2003@126.com

Key words: Nogo-A, cerebral ischemia, remyelination, Nogo extracellular peptide 1-40, growth-associated binding protein 43, microtubule associated protein 2

some neuronal populations (4,5). Researchers have presumed that neuronal Nogo-A may be involved in normal cell functioning different from the inhibitory role of oligodendroglial Nogo-A (6). To date, there is limited information concerning the distribution of Nogo-A in the intact and lesioned central nervous system (CNS), and the time-dependent changes of Nogo-A expression after damage to the CNS remain debatable. For example, Huber *et al* (7) failed to show a change in Nogo-A protein after cortical lesions in rats. By contrast, Zhou *et al* (8) demonstrated that the expression of Nogo-A was significantly increased at 6 h, lasting for 7 days in global ischemic rats. Eslamboli *et al* (9) reported the increased level of Nogo-A up to 2 months following cerebral ischemia in marmoset monkeys. However, the change of Nogo-A levels has not been well studied in the middle cerebral artery occlusion (MCAO) model. Therefore, the purpose of the present study was to systemically investigate the expression pattern of Nogo-A at different time points from days 1 to 28 after focal cerebral ischemia.

Nogo-A binds to the Nogo receptor (Ng-R) to activate intracellular signaling pathways, resulting in growth cone collapse that contributes to the failure of axon regeneration (10). This inhibition can be reversed by an anti-Nogo-A antibody (3). Previously, available data has attempted to elucidate that inhibition of Nogo-A may promote extensive growth of axons and behavioral recovery after injury (11). However, the exact mechanism underlying Nogo-A failure in myelin repair remains unclear. Brain plasticity has been demonstrated to occur following experimental injury (12), but no previous reports have evaluated the effect of myelin inhibitors on post-ischemic plasticity. Growth-associated binding protein 43 (GAP-43) is a nervous system-specific protein and considered to be an intrinsic determinant of axonal plasticity (13,14). When the nervous system is damaged, GAP-43 expression increases until the establishment of complete synaptic connections (15). A previous *in vivo* study reported that the expression of GAP-43 is upregulated in vulnerable brain lesions after hypoxia injury (16). The elevated expression of GAP-43 caused by injury may contribute the regenerative response of axonal damage and compensate for brain damage. Microtubule-associated protein 2 (MAP-2) is a cytoskeletal protein that serves a role in the growth, differentiation and plasticity of neurons (17). Several studies have reported a decrease in MAP-2 expression after ischemia (18), which suggests that MAP-2 is sensitive to ischemic injury and loss of MAP-2 leads to neuronal dysfunction and dendritic breakdown (19). Therefore, the expression levels of GAP-43 and MAP-2 are considered to be the preferred probe for studying neural and axonal plasticity. In the present study, to elucidate a potential molecular mechanism underlying the Nogo-A inhibitor, Nogo extracellular peptide 1-40 (NEP1-40), on myelin repair, the changes in GAP-43 and MAP-2 expression associated with brain plasticity in ischemic model rats were investigated. Therefore, the results of the present study may provide an insight for the treatment of poststroke deficits by targeting Nogo-A to promote CNS regeneration through enhancement of neuroanatomical plasticity.

Materials and methods

MCAO model establishment. Adult male Sprague-Dawley rats (n=146; weight, 260-280 g; age, 6-8 weeks) were purchased from the Department of Experimental Animal Sciences, Dalian Medical University. The animals were housed in pairs in standard cages with free access to food and water under a 12/12-h light/dark cycle and in standard laboratory conditions (temperature, 20-25˚C; relative humidity, 50-70%). Efforts were made to minimize the discomfort of the animals. All animal-related experiments were approved by the Animal Welfare Committee of Dalian Medical University (Dalian, China; approval number, 202106101) and followed the guidelines for Animal Care and Use adapted from the National Institutes of Health (20).

MCAO was performed as described by Longa *et al* (21). The rats were anesthetized by the intraperitoneal injection of 10% chloral hydrate (300 mg/kg). No signs of peritonitis or pain/discomfort were observed following the injection of 10% chloral hydrate. After median incision of the neck skin, the right common carotid artery (CCA), external carotid artery (ECA) and internal carotid artery (ICA) were carefully isolated from the surrounding nerves. Briefly, no. 4-0 nylon monofilament suture was inserted into the ECA and advanced into the ICA to block the origin of the right middle cerebral artery (MCA). The suture was inserted 18-20 mm beyond the origin of the ICA. At 2 h after MCAO, the intraluminal filament was carefully removed. Rats without left forelimb paresis or circling towards the left side were regarded as unsuccessful models and were excluded from further experiments. Sham control rats underwent surgery procedures without filament insertion.

Experimental group and drug stereotactic delivery. A total of 134 rats were established by MCAO for 2 h, eight rats died primarily due to the trauma of the surgery and six rats failed to induce successful model establishment. Successful ischemic rats were randomly allocated into three groups: i) MCAO model group (n=60, 30 for immunostaining and 30 for western blotting); ii) MCAO + saline group (received saline; n=30 for immunostaining); and iii) MCAO + NEP1-40 group (received NEP1-40; n=30 for immunostaining). Rats of each group were divided into the following five subgroups by the days of observation: Days 1, 3, 7, 14 and 28 (n=6 each time point). At days 1, 3 and 14 after transient MCAO, rats were anesthetized by the intraperitoneal injection of 10% chloral hydrate (300 mg/kg) and placed on a stereotaxic apparatus. A 2.0-mm hole was drilled through the skull, and a 10 μl solution containing 10 μg/μl NEP1-40 or an equal volume of saline was microinjected into the right lateral ventricle (coordinate, 0.8 mm anterior to the bregma, 1.3 mm lateral to the midline, 3.5 mm beneath the dura) at a rate of 0.05 μl/min for 10 min using a Hamilton microsyringe (10 μl syringe Hamilton 900 series). After finishing the injection, the needle was left in place for an additional 10 min to prevent reflux and slowly withdrawn over 5 min. Penicillin was used to prevent the wound from infection. After NEP1-40 microinjection, six rats died, which was most likely due to aseptic inflammation. Animals that did not receive an injection and only received sham operations were used as controls (n=12, six for immunostaining and six for western blotting). The general state of health of the animals was observed daily. When the rats exhibited body weight loss, reduced activity, or showed signs of pain, distress or discomfort, it was determined that humane endpoints had

been reached and the animals were euthanized before the end of experiment. At 12 h after NEP1-40 administration, the rats were anaesthetized by the intraperitoneal injection of 10% choral hydrate, then sacrificed by decapitation or cervical dislocation on the observation time points. Animal death was verified by cessation of carotid artery beats. Subsequently, the brain tissues were collected for further assessment.

Luxol fast blue (LFB) and Bielschowsky silver staining. LFB and Bielschowsky silver staining were performed as previously described (22). Brain tissues were resected, embedded in paraffin blocks, cut into continuous coronal sections of 5 μm thickness, and then stained with LFB or Bielschowsky silver. In brief, for LFB staining, sections were stained with 0.1% LFB solution for 10 h at 60˚C, washed with distilled water, then placed in 95% alcohol for 10 min. The slides were differentiated with 0.05% lithium carbonate for 10-30 sec and then rinsed in 70% alcohol solution for 20 sec. The differentiation step was repeated until the gray matter became colorless and the white matter remained blue.

For Bielschowsky silver staining, brain sections of striatum were placed in 20% silver nitrate at 37˚C in the dark for 25 min, followed by rinsing with distilled water. Ammoniacal silver solution was then added dropwise to the slices. After rinsing with water, slices were immersed in 10% formaldehyde for 10 min at 25˚C. Finally, the sections were fixed in 5% sodium thiosulfate for 5 min at 25˚C. Images were acquired in the lesioned striatum using a light microscope (Olympus Corporation; magnification, x200). Image-Pro Plus software (version 6.0; Media Cybernetics, Inc.) was used to calculate the staining density to quantify the damage of white matter nerve fibers.

Immunohistochemical staining. Following the establishment of successful euthanasia, immunohistochemistry was performed. Rats were perfused through the aorta with 200 ml normal saline, followed by 300 ml 4% paraformaldehyde (PFA; pH 7.4). The brains were removed, post-fixed in 4% PFA for 20-24 h at 25˚C and then dehydrated in 30% sucrose. The brain sections were cut into 5-μm thick serial sections with a cryostat (Cryocut 1800; Leica Microsystems, Inc.) and mounted on gelatin/chrome alum-coated glass slides. The slides were processed for Nogo-A, myelin basic protein (MBP), GAP-43 and MAP-2 staining using the avidin-biotin technique as described by Tu *et al* (23). Sections were blocked with 2% normal goat serum (OriGene Technologies, Inc.) for 30 min at 37˚C, and then incubated with a primary polyclonal antibody against Nogo-A (1:400; catalog no. AB5664P; Chemicon International; Thermo Fisher Scientific, Inc.), rabbit anti-MBP (1:750; catalog no. BA0094; Wuhan Boster Biological Technology, Ltd.), rabbit anti-GAP-43 (1:800; catalog no. sc-17790; Santa Cruz Biotechnology, Inc.) and rabbit anti-MAP-2 (1:500; catalog no. sc-3279; Santa Cruz Biotechnology, Inc.) overnight at 4˚C. After washing with PBS, sections were incubated with goat anti-mouse or goat anti-rabbit secondary antibodies conjugated to HRP (1:100; catalog nos. SP9001 or SP9002; OriGene Technologies, Inc.) for 30 min at 37˚C. The sections were thereafter rinsed and then processed with diaminobenzidine (1 mg/ml; 0.001% H_2O_2) for 2 min at 25˚C. The stained sections were viewed and images acquired using a light microscope at x100 magnification (Olympus Corporation).

MetaMorph software (version 7.8; Molecular Devices, LLC) was used for the quantification of cell numbers. A region with 1,400 μm width and 1,200 μm length in the ischemic striatum was defined for counting Nogo-A^+ cells. The slide was viewed at x100 magnification in a blinded manner. For each brain, four slides were obtained from 20-μm thick coronal sections between 1.4 mm anterior and 0.4 mm posterior to the bregma. All counts were pooled together and results are expressed as the average number per rat.

For the analysis of MBP, GAP-43 and MAP-2 optical density in the ischemic striatum of saline- or NEP1-40-treated rats, four non-continuous brain slides from each brain were obtained. For each slide, four high-power fields under x100 magnification were randomly selected. MetaMorph software was used for the quantification of average intensity in the region of the ischemic striatum. The average intensity was defined as the difference between the average gray value of a chosen field within the ischemic striatum and its background (24).

Western blotting. The ischemic striatum of the brain was removed and quickly placed into -196˚C liquid nitrogen. Frozen tissues were homogenized in homogenization buffer (50 mmol/l^{-1} Tris base, 2 mmol/l^{-1} EDTA, 40 mmol/l^{-1} NaF, 1 mmol/l^{-1} phenylmethylsulfonyl fluoride). The concentration of protein was quantified using the bicinchoninic acid assay kit. Proteins (60 μg) were separated via 10% SDS-PAGE gel and transferred onto a PVDF membrane. The membranes were blocked with 5% non-fat milk for 1 h at 25˚C and then incubated with a rabbit polyclonal Nogo-A antibody (1:2,000; catalog no. AB5664P; Chemicon International; Thermo Fisher Scientific, Inc.) overnight at 4˚C. After washing with TBST (0.05% Tween-20), the membranes were incubated with a goat anti-mouse or goat anti-rabbit IgG secondary antibody at 4˚C (1:1,000; catalog nos. sc-2005 or sc-2004; Santa Cruz Biotechnology, Inc.) for 1 h and then detected with ECL reagent (Santa Cruz Biotechnology, Inc.). The blots were then exposed to X-ray sensitive films for 1-5 min. Mouse anti-rat β-actin primary antibody (1:8,000; sc-47778; Santa Cruz Biotechnology, Inc.) served as the loading control.

Blots were scanned with Scanwizard (version 5.0; ScanWizard, Inc.) and band densities (Nogo-A and β-action) were measured using TotalLab software (version 1.0; Leica Microsystems GmbH). Values for Nogo-A were standardized based on the intensity of β-actin and expressed as the fold of control.

Neurological behavior assessment. Animal health was determined every day throughout the experiment. The rats were subjected to neurological tests at days 1, 3, 7, 14 and 28 following MCAO and treatment with saline or NEP1-40. Neurological deficit scores were analyzed as described previously (25), using modified neurological severity score (mNSS). mNSS is a composite of motor, sensory, reflex and balance tests. Neurological function was graded on a scale of 0-18 (normal, 0; maximal deficit score, 18). The higher the score, the more severe the injury. All experiments were conducted in a blinded manner.

Statistical analysis. The experiments were repeated three times. Data are expressed as the mean ± SEM. Statistical analyses were performed using GraphPad Prism 5.0 (GraphPad

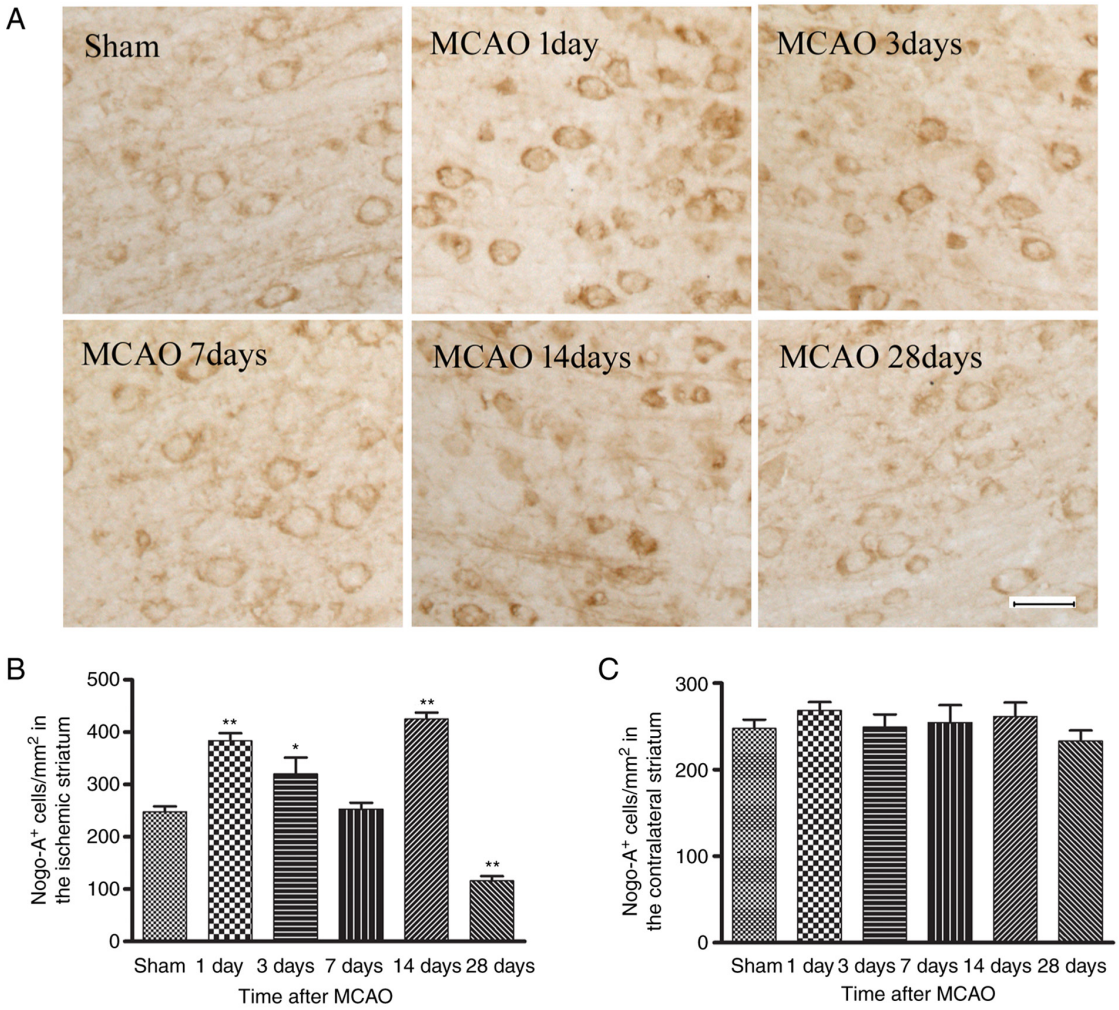

Figure 1. Immunohistochemical staining of Nogo-A in ischemic brain tissues. (A) Representative images of sections stained with anti-Nogo-A at days 1, 3, 7, 14 and 28 after MCAO (scale bar, 30 μm). (B) Quantification of the number of Nogo-A$^+$ cells in the ischemic brain at different time points. (C) Statistical analysis of Nogo-A$^+$ cells in the contralateral striatum. *P<0.05 and **P<0.01 vs. sham. MCAO, middle cerebral artery occlusion.

Software, Inc.). The data presented in Figs. 1-3 were analyzed using one-way ANOVA followed by Dunnett's post hoc test. The data presented in Figs. 4 and 5 were analyzed using one-way ANOVA followed by Tukey's post hoc test or two-way ANOVA followed by Tukey's post hoc test. The data presented in Fig. 6 were analyzed using one-way ANOVA followed by Tukey's post hoc test or mixed two-way ANOVA followed by Tukey's post hoc test. P<0.05 was considered to indicate a statistically significant difference.

Results

Time course of Nogo-A immunoreactivity after MCAO. A representative example of immunostaining for Nogo-A immunoreactivity in the right striatum of the sham-operation group (control) and on days 1, 3, 7, 14 and 28 after MCAO is presented in Fig. 1A. The Nogo-A immunoreactivity was located primarily in the cytoplasm of oligodendrocytes (small cell bodies and few processes) and observed predominantly in white matter tracts, typically found in parallel rows. Compared with the sham group, the number of Nogo-A immunoreactive cells was significantly elevated from day 1 to 3 post-stroke, then nearly returned to the control level at day 7, significantly

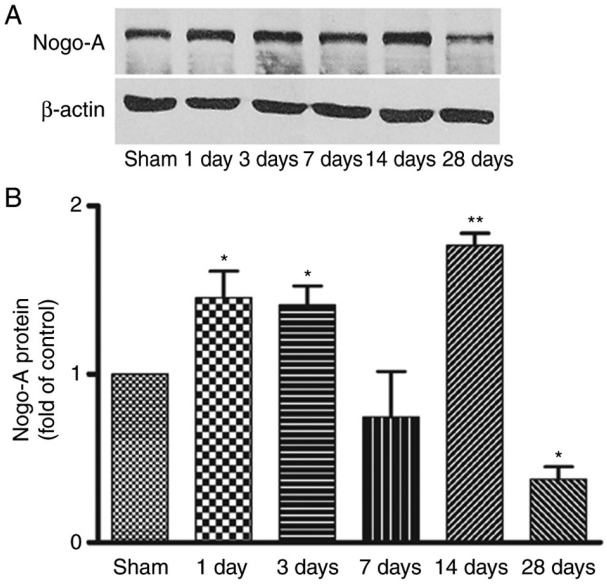

Figure 2. Western blot analysis of Nogo-A in the ischemic striatum after MCAO. (A) Nogo-A bands in the sham group and at different time points (days 1, 3, 7, 14 and 28 following MCAO) in the striatum. (B) Semi-quantification of the western blotting results. *P<0.05 and **P<0.01 vs. sham. MCAO, middle cerebral artery occlusion.

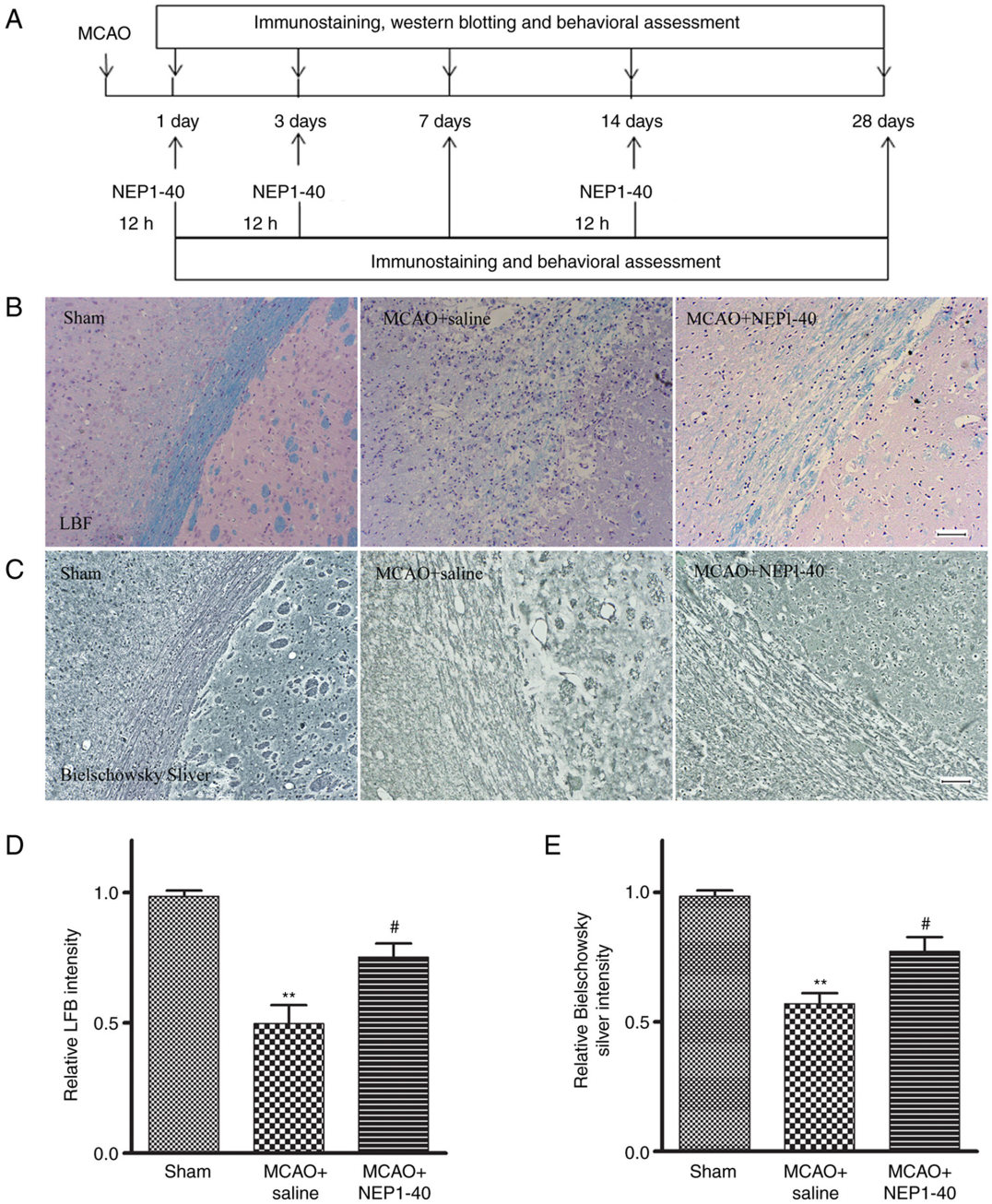

Figure 3. Representative images showing LFB and Bielschowsky silver staining in sham, saline-treated or NEP1-40-treated rats at day 7 after MCAO. (A) Experimental design. Representative image of (B) LFB and (C) Bielschowsky silver staining. Quantification of (D) LFB and (E) Bielschowsky silver staining. Scale bar, 50 μm. **P<0.01 vs. sham; $^{\#}$P<0.05 vs. MCAO + saline. MCAO, middle cerebral artery occlusion; LFB, Luxol fast blue; NEP1-40, Nogo extracellular peptide 1-40.

increased again at day 14, but then significantly decreased at day 28 in MCAO model rats (Fig. 1B). However, there was no significant change in the number of Nogo-A immunopositive oligodendrocytes between sham and MCAO model rats in the contralateral striatum at any time point (Fig. 1C), which suggested that the greatest inhibitory effect of Nogo-A may be exerted in the white matter areas immediately adjacent to the lesion.

Western blot analysis of Nogo-A expression in the striatum after MCAO. Representative bands of Nogo-A protein in the ischemic striatum from day 1 to day 28 after focal cerebral ischemia and the corresponding β-actin bands are shown in Fig. 2A. Consistent with the immunohistochemistry findings, compared with the sham group, Nogo-A expression was significantly increased from day 1 to day 3 following focal ischemia, returned to basal levels at day 7, then significantly elevated again at day 14 and significantly decreased at day 28 (Fig. 2B). This indicated that changes in Nogo-A expression were time-dependent following ischemia. However, no difference of Nogo-A protein was detected in the contralateral striatum at any time point (data not shown).

Effects of NEP1-40 on myelin repair in MCAO model rats. To investigate the effect of Nogo-A inhibitor NEP1-40 on the extent of demyelination in the white matter of MCAO

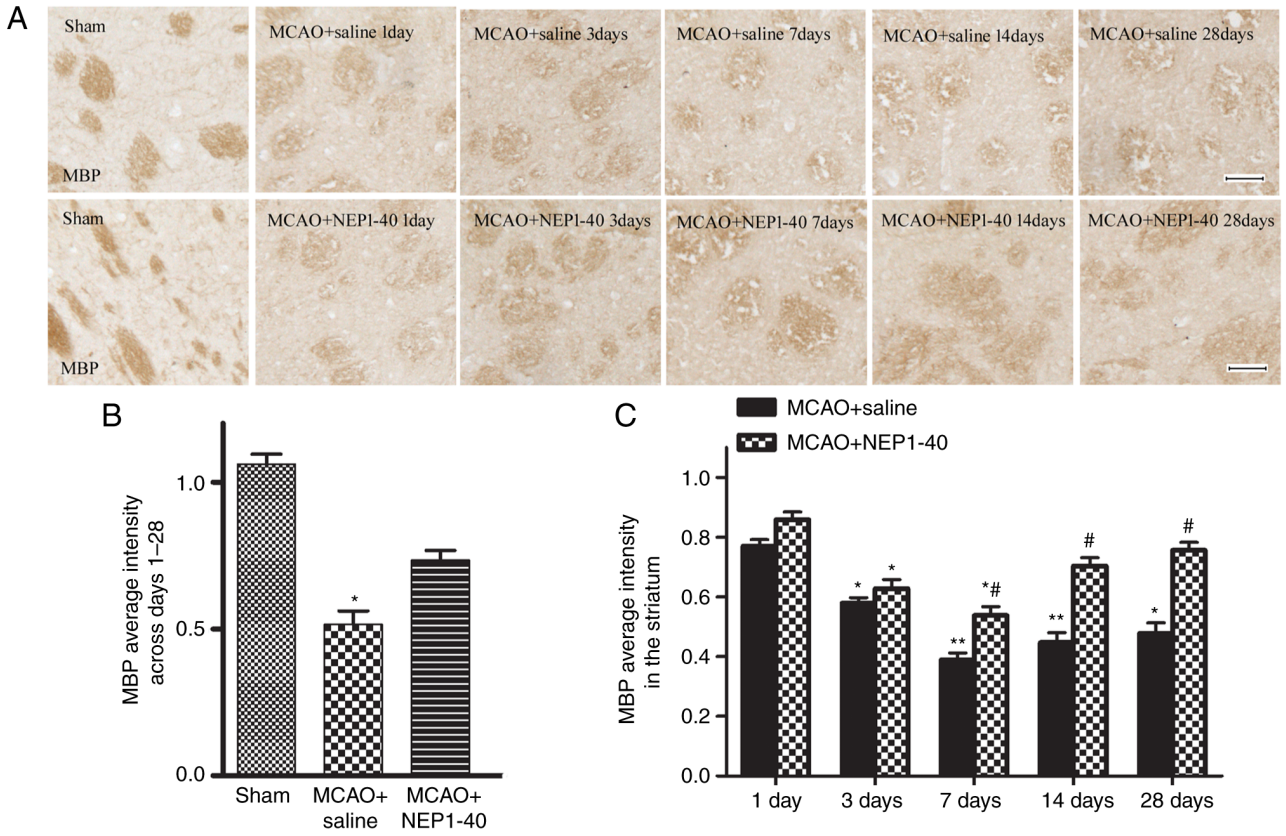

Figure 4. Effects of NEP1-40 on MBP expression as determined via immunohistochemistry. (A and B) Representative images of sections stained with anti-MBP antibody of the sham, MCAO + saline and MCAO + NEP1-40 groups at days 1, 3, 7, 14 and 28 after MCAO (scale bar, 50 μm). (C) Quantification of MBP intensity. MBP immunoreactivity in the ipsilateral striatum was decreased after MCAO from day 3 to day 28, which was notably restored by NEP1-40 treatment. *P<0.05 and **P<0.01 vs. sham or day 1; $^{\#}$P<0.05 vs. MCAO + saline. MCAO, middle cerebral artery occlusion; NEP1-40, Nogo extracellular peptide 1-40; MBP, myelin basic protein.

model rats, LFB, Bielschowsky silver staining and MBP immunohistochemistry were performed to assess the post-ischemic densities of myelinated axons in the striatum (Fig. 3A). LFB immunostaining was performed to assess the loss of myelin in sham, saline-treated and NEP1-40-treated rats at day 7 after MCAO (Fig. 3B and D). In the sham group, myelin exhibited a highly organized and compact appearance. In the MCAO + saline group, brain tissues exhibited a loose structure with disrupted morphology, and the staining intensity was significantly reduced compared with that in the sham group. In the MCAO + NEP1-40 group, the morphological changes were reduced compared with those in the saline-treated rats, whereas the staining intensity was significantly increased compared with that in the MCAO + saline group.

Bielschowsky silver is a marker for axons. Enhanced Bielschowsky silver staining has been correlated with axonal regrowth in rodent brains following MCAO (22). Thus, Bielschowsky silver staining was performed to assess axonal loss (Fig. 3C and E). In the sham group, the nerve fibers around the striatum were arranged closely and orderly. In the MCAO + saline group, the nerve fibers were disordered, suggesting there was white matter damage, and the staining intensity was significantly reduced compared with that in the sham group. NEP1-40 treatment inhibited these MCAO-induced effects. These data indicated that NEP1-40 treatment significantly reduced the extent of both myelin and axon loss after MCAO.

MBP, a major constituent of CNS myelin, has been used as a marker of post-ischemic white matter injury and repair (1). Accordingly, demyelination was also observed in the same region of white matter by immunostaining evaluation of MBP in the present study. Representative images of the time course of MBP staining in affected striatal tissues of rats in the MCAO + saline and MCAO + NEP1-40 groups are shown in Fig. 4A and B. A number of myelinated fibers, which were detected with the anti-MBP antibody, were clearly visible in the cerebral striatum of the sham group and each fiber tract could be easily followed. By contrast, these fibers became obscure and spaces between fiber tracts appeared during reperfusion following MCAO. Following NEP1-40 administration, the extent of myelin damage was slightly recovered in the ischemic area. The ratio of MBP optical density on the ischemic side was also analyzed (Fig. 4C). The average intensity of MBP immunoreactivity in the MCAO + saline group gradually decreased from day 1 to day 7, and marginally recovered at days 14 and 28. However, the difference between days 14 and 28 was not statistically significant. In addition, MBP expression was significantly restored by NEP1-40 treatment at days 7, 14 and 28 after MCAO compared with the MCAO + saline group. These results demonstrated that the myelin sheaths progressively deteriorated after ischemia, and blocking Nogo-A activity partially enhanced the extent or efficiency of endogenous remyelination.

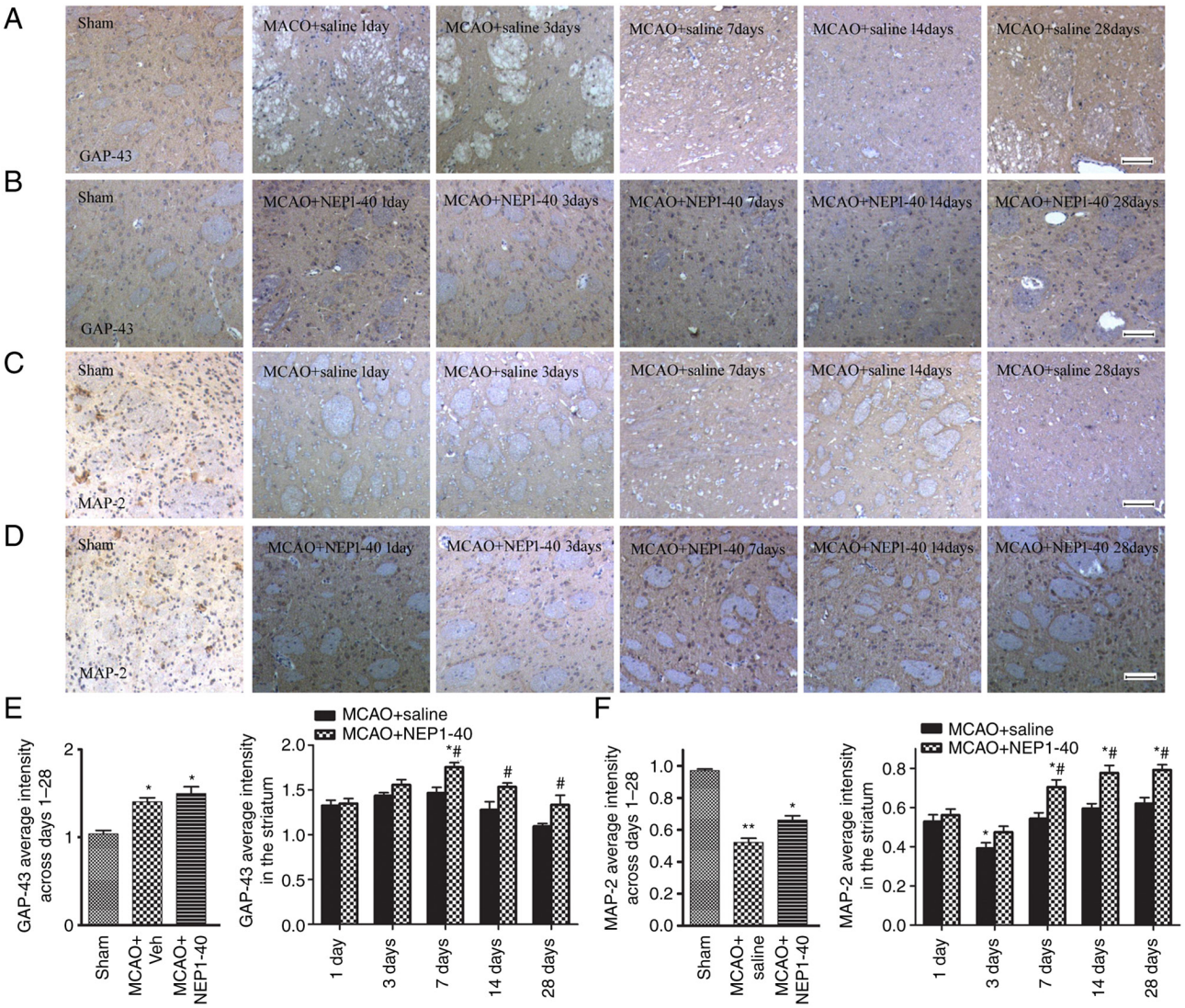

Figure 5. Effects of NEP1-40 on the expression of GAP-43 and MAP-2 as determined via immunohistochemistry. Representative images of (A and B) GAP-43 and (C and D) MAP-2 expression in the ipsilateral striatum of the sham, MCAO + saline and MCAO + NEP1-40 groups at days 1, 3, 7, 14 and 28 following MCAO (scale bar, 50 μm). Quantitative analysis of (E) GAP-43 and (F) MAP-2 expression in the ipsilateral striatum. *P<0.05 and **P<0.01 vs. sham or day 1; $^{\#}$P<0.05 vs. MCAO + saline. MCAO, middle cerebral artery occlusion; NEP1-40, Nogo extracellular peptide 1-40; GAP-43, growth-associated binding protein 43; MAP-2, microtubule associated protein 2.

Effects of NEP1-40 on GAP-43 and MAP-2 expression after MCAO. To further confirm a possible mechanism underlying the remyelinated effect mediated by Nogo-A inhibition, the expression levels of GAP-43 and MAP-2, which are molecular indicators of axonal plasticity in the CNS, were determined (13,17). GAP-43, an important promoter of axonal outgrowth (14), was detected via immunohistochemistry. Representative images of GAP-43 staining in the striatum of the MCAO + saline and MCAO + NEP1-40 groups are shown in Fig. 5A and B. In the sham group, GAP-43^{+} staining was brown and present in the axons and cytoplasm of neurons. After MCAO, GAP-43^{+} staining was observed in the ipsilateral striatum. The increase of GAP-43^{+} staining was markedly pronounced from day 1 to day 14, and declined to a baseline level at day 28 after ischemia (Fig. 5E). Treatment with NEP1-40 further increased the expression of GAP-43 at days 7, 14 and 28 after MCAO. These data indicated that the increase in GAP-43 expression may be closely related to injury repair and NEP1-40 may enhance the regenerative response in the damaged area.

MAP-2 is primarily associated with microtubules in the dendrite structure and is a sensitive marker of neuronal dysfunction (19). Thus, the expression of MAP-2 in the striatum of the ipsilateral hemisphere in saline- and NEP1-40-treated MCAO model rats was also examined by immunohistochemical staining (Fig. 5C and D). MAP-2 immunoreactivity stained brown was located exclusively in both the soma and dendrites of the neuron. After MCAO, distorted and disrupted axons alone with extensive loss of MAP-2 immunoreactivity in the striatum were observed, indicating that MAP-2 was vulnerable to ischemic injury. Quantification of the MAP-2 average intensity was also analyzed (Fig. 5F). MAP-2 showed a progressive decrease from day 1 to day 3 after MCAO. After NEP1-40 administration, the decreased level of MAP-2 was increased at days 7, 14 and 28 compared with the levels observed in the saline-treated group, but still remained lower compared

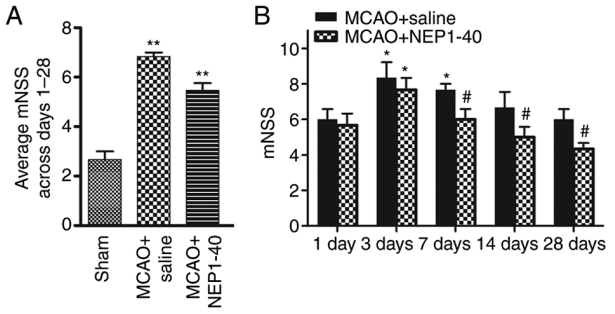

Figure 6. Effect of NEP1-40 administration on neurological scores. (A) mNSS were examined in saline- and NEP1-40-treated rats at days 1, 3, 7, 14 and 28 after MCAO. (B) Histogram represents the quantification of mNSS. *P<0.05 and **P<0.01 vs. sham or day 1; $^{\#}$P<0.05 vs. MCAO + saline. MCAO, middle cerebral artery occlusion; NEP1-40, Nogo extracellular peptide 1-40; mNSS, modified neurological severity scores.

with those in the sham group. These results suggested that Nogo-A inhibition prevented the loss of MAP-2^{+} dendrites and decreased neuronal damage.

Administration of NEP1-40 attenuates neurological deficits following ischemic stroke. To examine the effect of NEP1-40 treatment on behavioral function, the saline- and NEP1-40-treated MCAO model rats were examined using behavioral tests. After NEP1-40 treatment in the MCAO model rats, neurological performance was evaluated using mNSS at days 1, 3, 7, 14 and 28 after MCAO (Fig. 6). The behavior test showed that the neurological score in the saline-treated group was significantly increased compared with that in the sham group. In addition, in the MCAO + NEP1-40 group, neurological deficits were significantly reduced at days 7, 14 and 28 compared with those in the MCAO + saline group.

Discussion

Nogo-A is a major factor expressed in adult CNS myelin that mediates the inhibition of neurite regrowth and axonal regeneration (3). It has been reported that Nogo-A binds to the Ng-R to activate intracellular RhoA signaling pathways, resulting in growth cone collapse (26,27). In the present study, it was observed that Nogo-A^{+} cells were distributed throughout the white matter tract and primarily located in the cytoplasm of cells with oligodendroglial morphology, which was in agreement with a previous study (9). The localization of Nogo-A in oligodendrocytes was consistent with its role as a myelin-associated inhibitor of regenerative fiber growth and structural plasticity.

Next, a systematical observation regarding Nogo-A protein after MCAO was established via immunostaining and western blotting. Nogo-A expression began to increase at day 1 after MCAO, returning to the normal level at day 7. The alterations in Nogo-A expression during the first 7 days following ischemia were consistent with a previous study (8), but the present study did not observe the changes over a long-term period. The finding that Nogo-A expression increased at the early stages of ischemia suggested that it may serve an important role in preventing regeneration immediately following injury. In addition, the expression of Nogo-A increased again at day 14 after ischemia. It was hypothesized in the current study that this upregulation may prevent excessive axon regeneration, in particular oligodendrocyte proliferation, in response to injury. The expression of Nogo-A significantly decreased at day 28, leading to speculation that Nogo-A may be involved in the regulation of structural plasticity at the late phase of ischemia.

Increased Nogo-A expression after ischemic brain lesions can inhibit neurite outgrowth and fibroblast spouting (11), therefore treatment targeting Nogo-A could provide novel therapeutic strategies for nerve regeneration and repair. In the present study, it was found that MBP immunoreactivity staining significantly decreased across days 1-28 following ischemia, indicating that myelin loss occurred at an early time point (day 1) and advanced during ischemia. When the Nogo-A inhibitor was administered following MCAO, it was found that MBP expression significantly increased at day 7 to day 28 after MCAO, suggesting that NEP1-40 may promote remyelination and this protective effect occurred early at day 7 following ischemia. A previous study conducted by Zhu *et al* (28) also supported this result in ischemic neonatal rats. Other similar studies also showed that antibodies against Nogo-A (IN-1) and treatment with NEP1-40 resulted in the formation of new axonal connections and functional recovery (29). Nogo-A neutralization has been shown to improve behavioral outcomes and reduce neuronal damage in stroke model rats (30). Taken together, these results suggested that Nogo-A is a potent inhibitor of neurite growth involved in regenerative failure, and neutralization of Nogo-A may allow for the generation of nerve growth and enhance structural reorganization in regions surrounding the lesions. However, the underlying molecular mechanism remains to be elucidated. After cerebral ischemia, post-acute brain plasticity evolved as an important mechanism to maintain brain function (31,32). To investigate whether the enhanced regenerative processes mediated by Nogo-A inhibition were associated with post-traumatic plasticity, the effect of the myelin inhibitor NEP1-40 on MAP-2 and GAP-43, which are key markers of neuronal plasticity proteins (13,17), were determined.

GAP-43 is an intracellular membrane-associated phosphoprotein that is closely related to synaptic plasticity, axonal regeneration and neural sprouting (33). Studies have shown that in the early stage of nervous system development, GAP-43 content is increased in the neuronal cytoplasm (33,34). As the brain develops, GAP-43 expression gradually decreases; however, when brain injury occurs, its expression increases again until brain injury is repaired (14,35-36). Therefore, GAP-43 is regarded as an important marker for investigating nerve growth, development and repair. The findings of the current study revealed that GAP-43^{+} cells stained brown were present in the cytoplasm of neurons and were expressed at low levels in the brains of the sham group. After MCAO, the expression of GAP-43 in the ischemic striatum continuously increased from day 1 to day 14, then decreased to a baseline level at day 28. This observation coincided with a previous finding that the expression of GAP-43 in rat hippocampal neurons increases at the early phase of hypoxia (37). Furthermore, changes in the expression of GAP-43 have been found to be consistent with synapse formation over time (38), suggesting that GAP-43 may be involved in events such as axonal outgrowth and the process of myelin repair. Additional

previous studies have found further evidence for the notable role of GAP-43 in plasticity by demonstrating that increased GAP-43 synthesis is correlated with axonal remodeling and behavioral recovery (39-41). Additionally, in transgenic mice, overexpression of GAP-43 has been observed to lead to the spontaneous formation of new synapses and enhanced neuronal sprouting (42). The elevated expression of GAP-43 caused by ischemia in the early phase of MCAO may restore a microenvironment permissive for neuronal survival. As the time following injury increases, GAP-43 expression gradually decreases in the injured area, leading to the speculation that restored oligodendrocytes, decreased injured axons and myelin debris at the late stage of ischemia may in turn reduce GAP-43 expression. These findings support the fact that GAP-43 expression occurs during periods of accelerated spontaneous recovery and returns to baseline as recovery plateaus (38). Although ischemic injury can enhance GAP-43 expression to initiate a self-protection compensatory mechanism to a certain extent, this effect fails to fully repair the damaged myelin. Notably, in the present study GAP-43 expression significantly increased on days 1, 3, 7, 14 and 28 after NEP1-40 administration compared with that of saline-treated rats, which suggested that Nogo-A inhibition may have marked effects on white matter plasticity, and the repair of plasticity damage may be a novel mechanism of regeneration.

MAP-2 is a static structural protein, localized in neuronal somata and dendrites, that is necessary along with other cytoskeletal proteins to maintain neuroarchitecture (43,44). Previous investigations revealed dynamic functions for MAP-2 in the plasticity of neurons and synaptic activity. MAP-2 has been shown to be vulnerable to ischemic injury, and it is primarily speculated to be a specific marker of regeneration of axons and dendrites (45-49). In the present study, MAP-2 immunoreactivity was widely localized in the soma and dendrites of neurons, which had a smooth, regular appearance in the sham-operated control rats. After ischemia, the pattern of white matter in the MAP-2-stained sections showed a rough, globular appearance, indicating that ischemia induced damage to myelinated fiber tracts. The expression of MAP-2 was clearly reduced at day 1, reached a minimum at day 3 and slightly increased from day 7 to day 28, although the differences between days 7, 14 and 28 were not statistically significant. The loss of MAP-2 immunostaining during the early initial phase of cerebral ischemia indicated the collapse of cytoskeletal proteins and axonal disconnection. Despite the late partial increase in MAP-2, the expression failed to reach the levels observed in the sham group, suggesting that the intrinsic recovery mechanism was limited. NEP1-40 administration increased the expression of MAP-2^{+} dendrites in the damaged area and rescued neuronal survival. Increased and sustained MAP-2 expression may be an additional mechanism of overcoming myelin inhibition of axonal outgrowth. It is highly possible that the adaptive nature of the CNS environment mediated by Nogo-A inhibition may heighten structural plasticity and facilitate the process of axonal regeneration to some extent. However, the mechanism by which it changes in the MCAO model rat remains unknown.

In conclusion, the present data demonstrated that Nogo-A was localized in CNS myelin in a manner that was consistent with its described function as a neurite growth inhibitor. Moreover, the alterations in Nogo-A expression at different time points after MCAO and its potential role in regeneration were explored. Finally, it was revealed that NEP1-40 treatment at relevant time points post-injury may contribute to recovery and repair, most likely through compensatory increased levels of GAP-43 and MAP-2, which are speculated to be associated with brain plasticity. However, the precise mechanisms underlying the beneficial effects of Nogo-A inhibition in the presented experimental stroke model require further exploration.

Acknowledgements

The authors would like to thank Dr Yue Lu at the Peking University School of Nursing (Beijing, China) for their technical assistance.

Funding

This work was supported by grants from The National Natural Science Foundation of China (grant nos. 30570626, 81371355 and 81671191), The Beijing Natural Science Foundation (grant no. 7082028) and The Liaoning Revitalization Talents Program (grant no. XLYC 1807083).

Availability of data and materials

The datasets used and/or analyzed during the current study are available from the corresponding author on reasonable request.

Authors' contributions

HZ and YBZ conceived and designed the study, and finalized the manuscript. ZDL, XYG and XFW performed the experiments. CW and YL contributed to data collection and analysis. HZ drafted the manuscript. All authors have read and approved the final manuscript. HZ and ZDL confirm the authenticity of all the raw data.

Ethics approval and consent to participate

The animal-related experiments were approved by the Animal Welfare Committee of Dalian Medical University (Dalian, China) and followed the guidelines for Animal Care and Use adapted from the National Institutes of Health.

Patient consent for publication

Not applicable.

Competing interests

The authors declare that they have no competing interests.

References

1. Filbin MT: Myelin-associated inhibitors of axonal regeneration in the adult mammalian CNS. Nat Rev Neurosc 4: 703-713, 2003.
2. Baldwin KT and Giger RJ: Insights into the physiological role of CNS regeneration inhibitors. Front Mol Neurosci 8: 23, 2015.

3. Chen MS, Huber AB, van der Haar ME, Frank M, Schnell L, Spillmann AA, Christ F and Schwab ME: Nogo-A is a myelin-associated neurite outgrowth inhibitor and an antigen for monoclonal antibody IN-1. Nature 403: 434-439, 2000.
4. Liu H, Ng CE and Tang BL: Nogo-A expression in mouse central nervous system neurons. Neurosci Lett 328: 257-260, 2002.
5. Jin WL, Liu YY, Liu HL, Yang H, Wang Y, Jiao XY and Ju G: Intraneuronal localization of Nogo-A in the rat. J Comp Neurol 458: 1-10, 2003.
6. Llorens F, Gil V and del Río JA: Emerging functions of myelin-associated proteins during development, neuronal plasticity, and neurodegeneration. FASEB J 25: 463-475, 2011.
7. Huber AB, Weinmann O, Brösamle C, Oertle T and Schwab ME: Patterns of Nogo mRNA and protein expression in the developing and adult rat and after CNS lesions. J Neurosci 22: 3553-3567, 2002.
8. Zhou C, Li Y, Nanda A and Zhang JH: HBO suppresses Nogo-A, Ng-R, or RhoA expression in the cerebral cortex after global ischemia. Biochem Biophys Res Commun 309: 368-376, 2003.
9. Eslamboli A, Grundy RI and Irving EA: Time-dependent increase in Nogo-A expression after focal cerebral ischemia in marmoset monkeys. Neurosci Lett 408: 89-93, 2006.
10. Fournier AE, GrandPre T and Strittmatter SM: Identification of a receptor mediating Nogo-66 inhibition of axonal regeneration. Nature 409: 341-346, 2001.
11. Otero-Ortega L, Gómez-de Frutos MC, Laso-García F, Sánchez-Gonzalo A, Martínez-Arroyo A, Díez-Tejedor E and Gutiérrez-Fernández M: NogoA Neutralization promotes axonal restoration after white matter injury in subcortical stroke. Sci Rep 7: 9431, 2017.
12. Cheatwood JL, Emerick AJ and Kartje GL: Neuronal plasticity and functional recovery after ischemic stroke. Top Stroke Rehabil 15: 42-50, 2008.
13. Benowitz LI and Routtenberg A: GAP-43: An intrinsic determinant of neuronal development and plasticity. Trends Neurosci 20: 84-91, 1997.
14. Frey D, Laux T, Xu L, Schneider C and Caroni P: Shared and unique roles of CAP23 and GAP43 in actin regulation, neurite outgrowth, and anatomical plasticity. J Cell Biol 149: 1443-1454, 2000.
15. Emery DL, Raghupathi R, Saatman KE, Fischer I, Grady MS and McIntosh TK: Bilateral growth-related protein expression suggests a transient increase in regenerative potential following brain trauma. J Comp Neurol 424: 521-531, 2000.
16. Schmidt-Kastner R, Bedard A and Hakim A: Transient expression of GAP-43 within the hippocampus after global brain ischemia in rat. Cell Tissue Res 288: 225-238, 1997.
17. Matesic DF and Lin RC: Microtubule-associated protein 2 as an early indicator of ischemia-induced neurodegeneration in the gerbil forebrain. J Neurochem 63: 1012-1020, 1994.
18. Kitagawa K, Matsumoto M, Niinobe M, Mikoshiba K, Hata R, Ueda H, Handa N, Fukunaga R, Isaka Y, Kimura K, *et al:* Microtubule-associated protein 2 as a sensitive marker for cerebral ischemic damage-immunohistochemical investigation of dendritic damage. Neuroscience 31: 401-411, 1989.
19. Johnson GV and Jope RS: The role of microtubule-associated protein 2 (MAP-2) in neuronal growth, plasticity, and degeneration. J Neurosci Res 33: 505-512, 1992.
20. Zimmermann M: Ethical guidelines for investigations of experimental pain in conscious animals. Pain 16: 109-110, 1983.
21. Longa EZ, Weinstein PR, Carlson S and Cummins R: Reversible middle cerebral artery occlusion without craniectomy in rats. Stroke 20: 84-91, 1989.
22. Mao L, Jia J, Zhou X, Xiao Y, Wang Y, Mao X, Zhen X, Guan Y, Alkayed NJ and Cheng J: Delayed administration of a PTEN inhibitor BPV improves functional recovery after experimental stroke. Neuroscience 231: 272-281, 2013.
23. Tu H, Deng L, Sun Q, Yao L, Han JS and Wan Y: Hyperpolarization-activated, cyclic nucleotide-gated cation channels: Roles in the differential electrophysiological properties of rat primary afferent neurons. J Neurosci Res 76: 713-722, 2004.
24. Zhao H, Gao XY, Liu ZH, Lin JW, Wang SP, Wang DX and Zhang YB: Effects of the transcription factor Olig1 on the differentiation and remyelination of oligodendrocyte precursor cells after focal cerebral ischemia in rats. Mol Med Rep 20: 4603-4611, 2019.
25. Mao L, Huang M, Chen SC, Li YN, Xia YP, He QW, Wang MD, Huang Y, Zheng L and Hu B: Endogenous endothelial progenitor cells participate in neovascularization via CXCR4/SDF-1 axis and improve outcome after stroke. CNS Neurosci Ther 20: 460-468, 2014.
26. Huang S, Huang D, Zhao J and Chen L: Electroacupuncture promotes axonal regeneration in rats with focal cerebral ischemia through the downregulation of Nogo-A/NgR/RhoA/ROCK signaling. Exp Ther Med 14: 905-912, 2017.
27. Cao Y, Shumsky JS, Sabol MA, Kushner RA, Strittmatter S, Hamers FP, Lee DH, Rabacchi SA and Murray M: Nogo-66 receptor antagonist peptide (NEP1-40) administration promotes functional recovery and axonal growth after lateral funiculus injury in the adult rat. Neurorehabil Neural Repair 22: 262-278, 2008.
28. Zhu WW, Ma XL, Guo AL, Zhao HY and Luo HH: Neuroprotective effects of NEP1-40 and fasudil on Nogo-A expression in neonatal rats with hypoxic-ischemic brain damage. Genet Mol Res 10: 2987-2995, 2011.
29. Niederöst B, Oertle T, Fritsche J, McKinney RA and Bandtlow CE: Nogo-A and myelin-associated glycoprotein mediate neurite growth inhibition by antagonistic regulation of RhoA and Rac1. J Neurosci 22: 10368-10376, 2002.
30. Papadopoulos CM, Tsai SY, Cheatwood JL, Bollnow MR, Kolb BE, Schwab ME and Kartje GL: Dendritic plasticity in the adult rat following middle cerebral artery occlusion and Nogo-a neutralization. Cereb Cortex 16: 529-536, 2006.
31. Liu Q, Lv HW, Yang S, He YQ, Ma QR and Liu J: NEP1-40 alleviates behavioral phenotypes and promote oligodendrocyte progenitor cell differentiation in the hippocampus of cuprizone-induced demyelination mouse model. Neurosci Lett 725: 134872, 2020.
32. Boghdadi AG, Teo L and Bourne JA: The involvement of the myelin-associated inhibitors and their receptors in CNS plasticity and injury. Mol Neurobiol 55: 1831-1846, 2018.
33. Jacobson RD, Virag I and Skene JH: A protein associated with axon growth, GAP43 is widely distributed and developmentally regulated in rat CNS. J Neurosci 6: 1843-1855, 1986.
34. Hsu JY, Stein SA and Xu XM: Temporal and spatial distribution of growth-associated molecules and astroglial cells in the rat corticospinal tract during development. J Neurosci Res 80: 330-340, 2005.
35. Dijk F, Bergen AA and Kamphuis W: GAP-43 expression is upregulated in retinal ganglion cells after ischemia/reperfusion-induced damage. Exp Eye Res 84: 858-867, 2007.
36. Gregersen R, Christensen T, Lehrmann E, Diemer NH and Finsen B: Focal cerebral ischemia induces increased myelin basic protein and growth-associated protein-43 gene transcription in peri-infarct areas in the rat brain. Exp Brain Res 138: 384-392, 2001.
37. Gorup D, Bohaček I, Miličević T, Pochet R, Mitrečić D, Križ J and Gajović S: Increased expression and colocalization of GAP43 and CASP3 after brain ischemic lesion in mouse. Neurosci Lett 597: 176-182, 2015.
38. Zhu X, Wang P, Liu H, Zhan J, Wang J, Li M, Zeng L and Xu P: Changes and significance of SYP and GAP-43 expression in the hippocampus of CIH rats. Int J Med Sci 16: 394-402, 2019.
39. Masliah E, Fagan AM, Terry RD, DeTeresa R, Mallory M and Gage FH: Reactive synaptogenesis assessed by synaptophysin immunoreactivity is associated with GAP-43 in the dentate gyrus of the adult rat. Exp Neurol 113: 131-142, 1991.
40. Hulsebosch CE, DeWitt DS, Jenkins LW and Prough DS: Traumatic brain injury in rats results in increased expression of Gap-43 that correlates with behavioral recovery. Neurosci Lett 255: 83-86, 1998.
41. Ceber M, Sener U, Mihmanli A, Kilic U, Topcu B and Karakas M: The relationship between changes in the expression of growth associated protein-43 and functional recovery of the injured inferior alveolar nerve following transection without repair in adult rats. J Craniomaxillofac Surg 43: 1906-1913, 2015.
42. Aigner L, Arber S, Kapfhammer JP, Lauz T, Schneider C, Botteri F, Brenner HR and Caroni P: Overexpression of the neural growth-associated protein GAP-43 induces nerve sprouting in the adult nervous system of transgenic mice. Cell 183: 269-278, 1995.
43. Wiche G: High-Mr microtubule-associated proteins: Properties and functions. Biochem J 259: 1-12, 1989.
44. Dehmelt L and Halpain S: The MAP2/Tau family of microtubule-associated proteins. Genome Biol 6: 204, 2005.
45. Goodson HV and Jonasson EM: Microtubules and microtubule-associated proteins. Cold Spring Harb Perspect Biol 10: a022608, 2018.

46. Rosenstein JM: Diminished expression of microtubule-associated protein (MAP-2) and beta-tubulin as a putative marker for ischemic injury in neocortical transplants. Cell Transplant 4: 83-91, 1995.
47. Dawson DA and Hallenbeck JM: Acute focal ischemia-induced alterations in MAP2 immunostaining: Description of temporal changes and utilization as a marker for volumetric assessment of acute brain injury. J Cereb Blood Flow Metab 16: 170-174, 1996.
48. Li Y, Jiang N, Powers C and Chopp M: Neuronal damage and plasticity identified by microtubule-associated protein 2, growth-associated protein 43, and cyclin D1 immunoreactivity after focal cerebral ischemia in rats. Stroke 29: 1972-1980; discussion 1980-1, 1998.
49. Malinak C and Silverstein FS: Hypoxic-ischemic injury acutely disrupts microtubule-associated protein 2 immunostaining in neonatal rat brain. Biol Neonate 69: 257-267, 1996.